Title
Flexible and Accessible 4D Subsurface Visualization Using a Web-Based Platform

ISBN
9780979497575

Authors
Pratt, MJ
Knox, HA
Johnson, TC
et al.

Publication Date
2022

Peer reviewed

ARMA 22–2224

EGS Stimulation Design with Uncertainty Quantification at the EGS Collab Site

Burghardt, J., and Knox, H.A.
Pacific Northwest National Laboratory, Richland, Washington, USA
Doe, T.
TDoeGeo, Bellevue, Washington, USA
Blankenship, D., Schwering, P.C., and Ingraham M.
Sandia National Laboratories, Albuquerque, New Mexico, USA
Kneafsey, T.J., Dobson, P.F., Ulrich, C., and Guglielmi, Y.
Lawrence Berkeley National Laboratory, Berkeley, California, USA
Roggenthen, W.
South Dakota School of Mines and Technology, Rapid City, South Dakota, USA

This paper was prepared for presentation at the 56th US Rock Mechanics/Geomechanics Symposium held in Santa Fe, New Mexico, USA, 26-29 June 2022. This paper was selected for presentation at the symposium by an ARMA Technical Program Committee based on a technical and critical review of the paper by a minimum of two technical reviewers. The material, as presented, does not necessarily reflect any position of ARMA, its officers, or members. Electronic reproduction, distribution, or storage of any part of this paper for commercial purposes without the written consent of ARMA is prohibited. Permission to reproduce in print is restricted to an abstract of not more than 200 words; illustrations may not be copied. The abstract must contain conspicuous acknowledgement of where and by whom the paper was presented.

ABSTRACT: Engineering a robust hydraulic connection between wells is one of the most difficult aspects of enhanced geothermal systems (EGS). Designing and constructing such hydraulic connections requires an understanding of the in-situ state of stress and the heterogeneities and discontinuities that naturally exist and may control the stimulation. Even with comprehensive stress and formation characterization programs, substantial uncertainty remains in these key parameters. This is especially the case in high-temperature EGS environments where drilling conditions are often difficult and far fewer logging and testing options are available. This paper presents a new approach for explicitly quantifying the uncertainties in the state of stress using a Bayesian Markov Chain Monte Carlo method. This approach produces a probability distribution for the stress tensor, including a general 3D orientation, that reflects the uncertainties in all the observations or indicators used to constrain the stress state. This method is demonstrated using the characterization data for the EGS Collab Experiment 2 site. The output of the analysis is used to guide the design of the planned stimulations. In the case of research projects like EGS Collab, explicitly quantifying the uncertainties in the stress state allows for more rigorous hypothesis testing by allowing conclusions drawn from the experiments to be interpreted in the context of the uncertain knowledge about conditions in the test bed.

1. INTRODUCTION

Enhanced Geothermal Systems (EGS) require use of hydraulic pressure to artificially generate fluid pathways between one or more wells. The hydraulic pressure interacts with the in-situ state of stress and rock properties to create new fractures or enhance the permeability of existing fractures. The fracturing can include contributions from both tensile (Mode I) and shearing (Mode II) displacements (e.g., Norbeck et al., 2018). One concept for creating sustainable EGS reservoirs centers on preferentially creating Mode II shearing displacements on naturally occurring fractures, which is often called shear stimulation or "hydroshearing." The potential advantage to shear-mode stimulation is that when fractures shear, they often also permanently dilate because the asperities on the fracture faces no-longer mate together perfectly after the shearing offset. This has the potential to create a fracture with significantly improved hydraulic conductivity without requiring the placement of proppant as in petroleum stimulation operations.

In deep EGS settings high-fidelity interrogation of the behavior of individual fractures is generally not possible because of the limited options for logging tools and open-hole packers for EGS reservoirs approaching or exceeding 200 °C. Furthermore, no instruments have been operated at EGS depths and temperatures that can measure fracture displacements during stimulation. Therefore, the body of knowledge about the shear stimulation concept is limited to observations of hydraulic properties of relatively large depth intervals of open hole sections, often hundreds of meters, before and after stimulation. Furthermore, very accurate knowledge of the state of stress in EGS reservoirs is also usually lacking because of the same difficulties of availability of high-temperature tools.

Table 1. Measured stress indicators in well TV4100 for zones above the rhyolite dike; ISIP=instantaneous shut-in pressure; NT = not tested; AMB = ambiguous test results

Depth (m)	Initiation Pressure (MPa)	Hydraulic Reopening Pressure (MPa)	Sleeve Opening Pressure (MPa)	ISIP (MPa)	Flowback Closure Pressure (MPa)	Shut-in Closure Pressure (MPa)
9.6	25.1	23.8	NT	22.3	AMB	20.9
11.9	23.8	20.4	20.1	21.5	AMB	AMB
16.1	21.8	22.5	NT	22.7	AMB	21.5
19.7	22.4	18.6	NT	21.7	18.3	AMB
25.9	23.4	18.6	NT	20.0	18.4	19.5
28.4	22.1	18.3	NT	21.5	AMB	AMB

The objective of Experiment 2 of the EGS Collab project is to collect high-fidelity measurements of shear stimulation in an environment that is as close as possible to EGS conditions while also allowing measurements that cannot currently be made under EGS conditions. Experiment 1, now completed, focused on tensile fracture propagation and heat transfer. The Sanford Underground Research Facility (SURF) was chosen as the site for this experiment because it allows access to crystalline rock at stress conditions of the same order of magnitude as many potential EGS reservoirs. Because of the extensive system of drifts created during the operation of the former Homestake Gold Mine at SURF, it is possible to drill and access wells into such high stress conditions for relatively modest costs.

Several other papers being presented at this symposium offer a description of various aspects of this project and experimental test bed (Kneafsey et al, 2022, Ulrich et al, 2022). The objective of this paper is to present the analysis of the state of stress at the Experiment 2 test bed and how this information was used to design the stimulation program.

1.1. Stress observations

Table 1, modified from Burghardt et al. (2020), summarizes the results of the stress measurements made in zones in well TV4100 in the Yates amphibolite above the rhyolite dike intersected by the well. Well TV4100 was a vertical characterization well drilled from within a mine drift on the 4100 Level (approximately 4100 ft below ground surface). The stress measurements indicated significant differences in the stress field above, within, and below the rhyolite dike. Since all the wells being used for the stimulation and flow experiments on the 4100 Level are above the rhyolite dike, we will focus only on the measurements in this region. Table 2 lists the observed fracture orientations corresponding to the stress measurements listed in Table 1. An unexpected finding was that the induced fractured were inclined significantly from vertical. Many of these induced fractures appear to follow pre-existing fractures. Despite this, as the table shows, there was a high degree of consistency in the fracture dips and strikes. There are many fractures at varying orientations that appear similar to the ones that were opened by the fracturing. This suggests that these induced fracture orientations are indicative of a consistent stress direction trend at the site.

In addition to these indicators, another observation from borehole logs that is relevant to the state of stress is that no borehole breakouts or drilling-induced tensile fractures were observed in well TV4100. Absence of such features can be used to estimate limits on how large the difference between principal stresses are. However, this limit depends upon the stress at which the rock surrounding the borehole would fail in shear and localize sufficiently into shear bands that would form breakouts. Such failure and localization processes are difficult to predict because they are highly sensitive to the size and geometry involved. A typical approach is to use a laboratory-derived unconfined compressive strength (UCS) value. However, UCS is known to depend on the size and shape of the sample (Bažant and Planas, 1998, Masoumi, 2020) . Therefore, while this approach is useful, significant uncertainty remains in the rock strength and therefore in the bounds that can be placed on the principal stresses using the presence or absence of borehole failure modes. The method described below is intended to account for such uncertainties, making this information valuable but not uniquely determinative of the stress state.

Table 2. Observed induced fracture orientations in TV4100 for the zones above the rhyolite dike. Depth is measured depth below well collar, which is at approximately 4100 feet below ground surface.

Depth (m/ft)	Dip Trend	Dip	Confidence
9.6/31	176°	51°	20%
11.9/39	221°	56°	40%
16.1/53	207°	59°	60%
19.7/65	207°	68°	80%
25.9/85	200°	59°	80%
28.4/93	201°	63°	60%

2. METHODS

The stress indicators mentioned above all contain information about the state of stress at the EGS Collab Experiment 2 site. However, all these observations are subject to uncertainty. The relationship between the uncertain observed quantities and the principal stresses is relatively complex, especially in the case such as this where the principal stresses being out of alignment with the borehole direction is at least a possibility that should be considered. The method presented here is a means to integrate all these observations together while explicitly accounting for the uncertainty in each observation and relevant properties.

The method uses the Metropolis-Hastings Markov Chain Monte Carlo (MCMC) sampling scheme to compute the posterior probability distribution for the stress tensor and pore pressure. Under this scheme the principal stresses, their directions, the pore pressure, as well as various rock properties that are discussed below, are taken as random variables. Random variables in Bayesian statistics should be understood to mean that the true value of the variable is not perfectly known, not that the variable is randomly changing as in a frequentist statistical approach. The MCMC algorithm is a method for assembling samples from the posterior probability distribution of the group of random variables with respect to observations that are sensitive to the variables. The MCMC approach will be briefly outlined here to introduce the terminology that will be needed to explain how it is applied to the stress estimation problem. For a more detailed treatment the reader is referred to Gelman et al. (2004).

The MCMC approach is based on Bayes' law, which expresses the probability of distribution of a random variable, or collection of variables, X under the condition of an observation D:

$$P(X|D) = \frac{P(D|X)P(X)}{P(D)} \qquad (1)$$

$P(X|D)$ is referred to as the posterior probability distribution of X with respect to D. $P(D|X)$ is known as the likelihood function and is essential to the MCMC scheme. The likelihood function expresses the probability of the observation, D, if X were the true value. $P(X)$ is the prior probability distribution for X, reflecting the state of knowledge of X prior to the observation D. $P(D)$ is essentially a normalizing function that ensures that the posterior is properly normalized so that the integral of all possible values of X has a value of unity.

The Metropolis-Hastings MCMC scheme works by beginning from a point in the random variable space. The only constraint on the starting point is that the likelihood and posterior distributions must be defined. Beginning from this starting point each random variable is randomly perturbed by drawing values from a probability distribution called the proposal distribution, which is chosen for each variable. We will refer to this perturbed state as X'. For all variables a Gaussian proposal distribution with zero mean is used. The likelihood function is then evaluated at the perturbed state. The perturbed state is then accepted or rejected with a probability that is proportional to the ratio of the likelihood of the perturbed state and the state at the beginning of the iteration. This is done by computing the ratio of the likelihoods:

$$\alpha = \frac{P(D|X')}{P(D|X)} \qquad (2)$$

Then a uniform random number between zero and one, denoted u, is drawn. If $u \leq \alpha$ then X' is accepted, otherwise it is rejected. If X' is accepted, then it becomes the starting point for the next iteration. If it is rejected, then X is kept as the starting point for the next iteration and a new perturbation is selected.

Each section below derives the likelihood function for each observation relevant to the state of stress. Some of these observations involve rock properties, such as compressive strength, that are not perfectly known. Consistent with the Bayesian approach, these variables will be taken as random variables and assigned a prior distribution reflecting the state of knowledge of the variable before the observations in question are made. As these variables are included in the MCMC sampling, each will have a posterior distribution with respect to each observation.

In some where there are sufficient independent observations/pieces of evidence, these observations can help to constrain the relevant rock properties. Generally, however, with few independent observations the posterior distributions of uncertain rock properties and the state of stress are highly correlated such that the true value of the rock properties is not inferred independently.

2.1. Probabilistic representation of stress

Because stress is a tensorial quantity and statistical methods have been infrequently applied to tensorial quantities we will briefly explain how this is approached. A commonly used approach in the literature is to treat each component, or each principal value, as an independent variable (e.g., Chiaramonte et al., 2015). This is convenient since standard univariate statistical distributions and methods, such as Monte Carlo sampling, can be used.

However, in many cases there are correlations between the values of the stress components. This is especially true for the intermediate principal stress. This is because most of the methods used to constrain the intermediate principal stress, such as the presence or absence of borehole breakouts, are sensitive not to the intermediate principal stress itself but to the difference between the

minimum and intermediate principal stresses. Therefore, the value that would be expected for the intermediate principal stress depends on the value expected for the minimum principal stress, and therefore there is a strong correlation between the two variables.

Because of this, uncertainty in tensorial quantities should best be thought of as *joint* probability distributions between the components of the tensor. In the general case where the principal stress directions are arbitrary, it is then possible to represent the stress tensor as the joint distribution of the six independent stress components or as between the three principal stress components and their respective orientations. To apply the MCMC method we then need to begin with a prior probability distribution for the stress tensor, and then we need to derive likelihood functions for each of the stress indicators listed in Table 1 in terms of likelihood functions. Each of the subsections below briefly summarizes how the indicator is expressed statistically as a likelihood function.

2.2. Lithostatic stress magnitude and orientation

We will take as an assumption that the magnitude of one of these principal stresses can be calculated using the true vertical depth and average mass density of the overburden formations on the 4100 level, which is thought to be 35 MPa (5076 psi). Furthermore, a prior probability for the orientation of the lithostatic stress was prescribed using a Fischer/von Mises distribution with a mode of zero (vertical) and a shape parameter of 45. The effect this prior assumption has in the MCMC scheme is, all else being equal, to accept stress states where the lithostatic component of stress is close to vertical with a higher probability than stress states where it is further from vertical. This does not *require* the lithostatic stress to be vertical, but simply expresses a preference for vertical lithostatic stress components reflecting the fact that this is usually (but not always) the case.

2.3. Rock mass frictional strength

Another constraint on the magnitude of the difference between principal stresses is the recognition that faults and fractures are pervasive in the subsurface, and so the strength of these features limits the principal stress differences, leading to the concept known as the stress polygon (Zoback et al., 2003). A stochastic version of the stress polygon is included in the analysis, with the fault friction coefficient being taken as an uncertain parameter in the MCMC scheme. Figure 1 shows the probability distribution for the fault friction coefficient used to constrain the magnitude of the difference between the principal stresses. A lognormal distribution is used reflecting a most likely value of 0.6, with a rapidly decaying probability of larger and smaller values. The lognormal distribution has finite probabilities for only positive values, so negative values are not permitted as is physically reasonable.

The pore pressure also plays an important role in evaluating the stress states that are permissible. The pore pressure is highly uncertain at SURF, as widely different values have been observed only short distances away from each other (e.g., Stetler, 2015). On the 4100 level, well TV4100 built up approximately 200 psi when it was shut in, while all of the other wells drilled have been observed to lose water, indicating a pore pressure below atmospheric pressure. As such, the prior probability distribution for the pore pressure was chosen to be a uniform distribution between zero pressure (atmospheric) and hydrostatic pressure (15 MPa (2176 psi)), as shown in Figure 2.

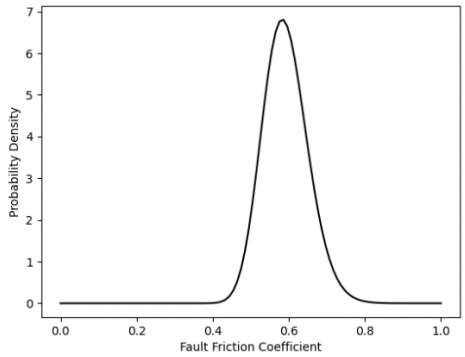

Figure 1. Probability density function used to describe the fault friction coefficient that limits the magnitude of the difference between principal stresses

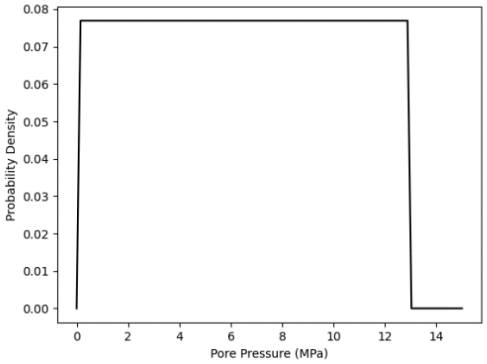

Figure 2. Prior probability density function for the pore pressure

2.4. Fracture closure pressure

The fracture closure pressure observations were summarized using a uniform probability distribution between 18.3 MPa (2654 psi) and 23 MPa (3336 psi), as shown in Figure 3. This is reflecting both the uncertainty in the methods used to estimate the fracture closure pressure for each test and the spatial variability of the stress within this region of the test bed, since we are seeking an estimate for the nominal stress state in this region. The validity of the analysis presented here is contingent upon the assumption that the tests conducted capture the extent of the real spatial variability. Since a finite number of tests were conducted it is possible that

the actual spatial variability of stress extends to outside of this range.

2.5. *Induced fracture orientation*

The induced fracture orientations are used to constrain the stress magnitude and directions. Figure 4 and Figure 5 show the probability distributions used to summarize the observed fracture orientations. This information is used in the MCMC sampling scheme in two different ways corresponding to two different hypotheses for the orientation of the induced fractures, as discussed in Section 3.1 and 3.2.

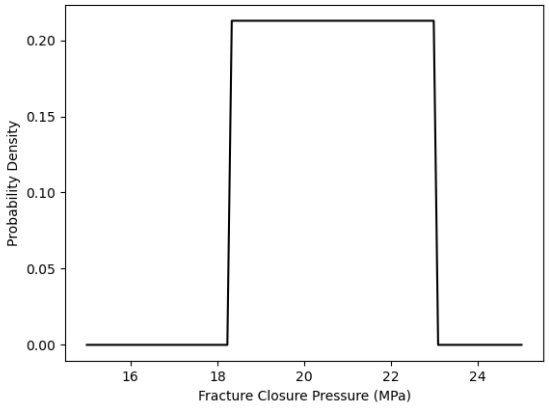

Figure 3. Plot of the probability distribution used to summarize the fracture closure pressure observations: a uniform distribution between 18.3 MPa (2654 psi) and 23 MPa (3336 psi)

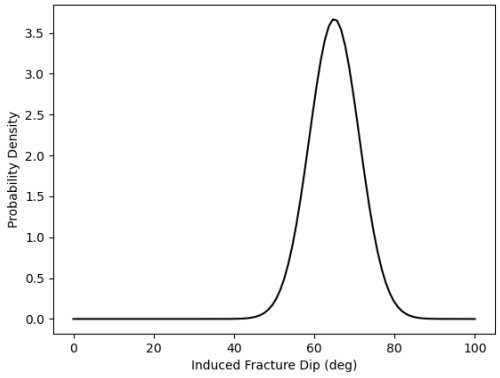

Figure 4. Probability distribution used to summarize the induced fracture dip angle: a Fischer/von Mises distribution with a mode of 65° and a shape parameter of 85.

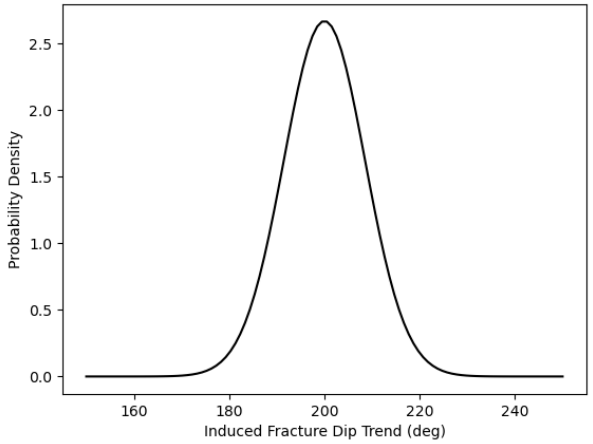

Figure 5. Probability distribution used to summarize the induced fracture dip trend angle (measured clockwise from true North): a Fischer/von Mises distribution with a mode of 200° and a shape parameter of 45.

2.6. *Sleeve fracture reopening pressure*

A sleeve fracture reopening test uses a packer placed over the fracture to reopen the fracture at the borehole. This ensures that pressure is only applied at the borehole wall and not within the fracture. This makes sleeve reopening tests more suitable to interpretation using a borehole stress solution than hydraulic reopening tests that can load the inside of the fracture if some residual hydraulic conductivity remains. These tests are very helpful to constrain the magnitude of the maximum subhorizontal principal stress. There was a single sleeve fracture reopening test performed in TV4100 at a depth of 11.9 m (39 ft).

The sleeve fracture reopening pressure is picked based on a change in slope of the pressure versus volume curve. As described in Burghardt et al (2020), this curve undergoes a gradual transition from low compliance to high compliance as the fracture opens. Thus, no unique value is possible to determine. Therefore, the sleeve fracture reopening pressure is represented with a uniform distribution with range of pressures consistent with this transition and is shown in Figure 6. This information is used in the MCMC sampling scheme in two different ways corresponding to two different hypotheses for the orientation of the induced fractures, as discussed below. The likelihood is then evaluated using the probability distribution shown in Figure 6. This essentially excludes stress states that have reopening pressures outside of 18-23.8 MPa but accepts any stress state with a reopening pressure in this range with equal probability.

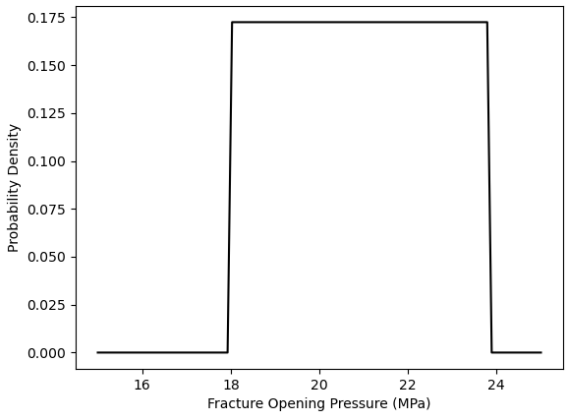

Figure 6. Plot of the probability distribution used to summarize the sleeve fracture reopening pressure observation: a uniform distribution between 18 MPa (2610 psi) and 23.8 MPa (3452 psi)

2.7. Absence of borehole breakouts

The absence of borehole breakouts in TV4100 can be used to place some constraint on the relative magnitude of the principal stresses. This constraint depends on the strength of the rock and the temperature and pressure history of the well between when it was drilled and logged. It is assumed that the pressure remained close to atmospheric and the temperature of the fluid inside the well remained very close to the formation temperature, so temperature gradients between the water used to drill the well and the formation played no role in the state of stress surrounding the well. The rock strength was characterized using a Mohr Coulomb failure criterion. The two parameters in this criterion were expressed in terms of the unconfined compressive strength (UCS) and the internal friction coefficient. The uniform probability distribution shown in Figure 7 for the UCS and a deterministic value for the internal friction coefficient of 0.2 was used.

The UCS was taken as a stochastic variable within the MCMC scheme, and the probability distribution shown in Figure 7 was used to compute the likelihood of any MCMC sample together with whether or not a breakout would be expected for a given value of the rock strength and principal stresses and orientations. Combinations of rock strength and stress parameters that would be expected to form breakouts (based on the compressive principal stresses surrounding the borehole) were rejected from the MCMC sampling scheme. This limits the difference in principal stress magnitudes but does so in a way that recognizes the uncertainty in the rock strength.

The formation of breakouts and drilling-induced tensile fractures is also sensitive to the drilling mud pressure, which in deep wells is often a source of significant uncertainty since transients in mud pressure occurring during circulation or tripping tools in/out of the well must be considered. In this case because the well was drilled a relatively short distance from within a mine drift using only water, the drilling "mud" pressure was never significantly different from atmospheric pressure and is therefore not subject to significant uncertainty and are taken as deterministic parameters. For cases where this is not the case the mud pressure and temperature can be represented as stochastic variables in a similar way to how UCS is considered here.

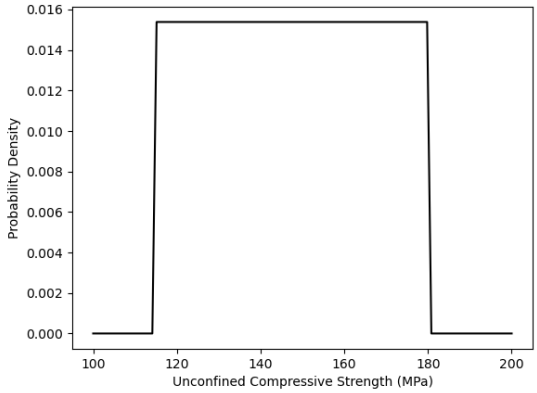

Figure 7. Probability density function for the unconfined compressive strength (UCS): a uniform distribution between 115 and 180 MPa

3. RESULTS

The stress indicators listed in Table 1 and observed fracture orientations listed in Table 2 were used with the MCMC method described in Section 2 to compute the probability distribution for the principal stress magnitudes and directions. For each of the two stress hypotheses a total of 100,000 MCMC sampling realizations were drawn with the fist 5,000 realizations being discarded, often called "burn-in", so as not to bias the results from the starting position. On a desktop computer these 100,000 realizations take a few minutes, so more realizations could easily be performed, though through an *ad hoc* estimation the results did not seem to change substantially with additional realizations. Formal MCMC convergence testing is planned in the future. This scheme uses elasticity solutions for the stress surrounding a borehole in a stress field with arbitrary principal stress magnitudes and directions, following the solutions in Peška and Zoback (1995). Each stress state realization from the MCMC run was also mapped to all of the fractures identified from image logs in well E2-TC, which is the well where stimulation is targeted in Experiment 2.

Two different hypotheses have been put forth to explain the induced fracture orientations being so far from the vertical orientation that is typically expected in the subsurface. The first is that the fractures are dipping because the minimum principal stress is dipping, and therefore the orientation where the stress is most tensile at the borehole wall is where the fractures formed. The second hypothesis is that there is a persistent plane of weakness in the rock, such as a natural fracture set, that makes the rock significantly weaker at the orientation where the fractures are observed. The MCMC analysis

was performed for both scenarios, as described below. The posterior probability distributions for both stress state hypotheses presented above were used to compute the shear and normal stress on the fractures observed in well E2-TC.

3.1. Stress-driven fracture orientation hypothesis

To reflect this hypothesis in the MCMC analysis, for each realization for the combination of sleeve fracture opening pressure and induced fracture orientation, the well pressure at which one of the principal stresses at the borehole wall becomes tensile is computed. The principal stresses at the borehole wall under this wellbore pressure are then computed. The likelihood of this orientation is computed by evaluating the induced fracture orientation probability distributions shown in Section 2.5 for the plane where the tensile stress occurs on the borehole wall. This results in high likelihoods for the combinations of stress orientations and magnitudes that produce tensile stresses at the borehole wall in the orientations consistent with the fracture orientations observed on the image logs.

As shown in Figure 9, the most likely value for the maximum subhorizontal stress under this hypothesis is approximately 35 MPa, which is equal to the lithostatic stress. The most likely azimuth of the minimum subhorizontal stress is 20° (Figure 10). The magnitude of the minimum subhorizontal stress is essentially equal to the uniform likelihood distribution used to summarize the closure pressure distirubtion (Figure 3), and therefore lacks a district maxima. The most likely deviation of the subvertical stress, which also corresponds to the dip of the minimum subhorizontal stress, is approximately 12°.

Using these most likely values for the principal stresses and directions, the expected stress state around the circumference of E2-TC at various well pressures were computed and are shown in Figure 8. The circumferential angle around the borehole is measured from the bottom of the well, so that an angle of 180° is the top of the well. The angle ω, plotted with the dashed black line and shown on the right-hand axes, is the angle of the minimum tangential principal stress measured from a plane perpendicular to the well axis, measured as a counterclockwise rotation about the radial vector with zero being toward the downward axis of the well. This means that $\omega = 0°$ would represent the case where the minimum tangential stress is oriented along the length of the well, which would produce a transverse fracture when $\sigma_{\theta 2}$ exceeded the tensile strength of the rock. Similarly, $\omega = 90°$ would represent the case where the minimum tangential stress, $\sigma_{\theta 2}$, is oriented exactly perpendicular to the well such that when it exceeded the tensile strength of the rock a longitudinal fracture would form.

The plots in Figure 8 indicate that a fluid pressure of 53.5 MPa (7760 psi) would be required to begin producing tensile tangential stresses on the surface of the borehole. Additional pressure above this value would be required to overcome the tensile strength of the rock and produce a fracture. With a fluid pressure of 53.5 MPa (7760 psi) where the tangential stress begins to become tensile the location of the tensile component of stress is within a few degrees of the top and bottom of the well and the orientation of the tensile component of stress is 150° with respect to a plane perpendicular to the well. This means

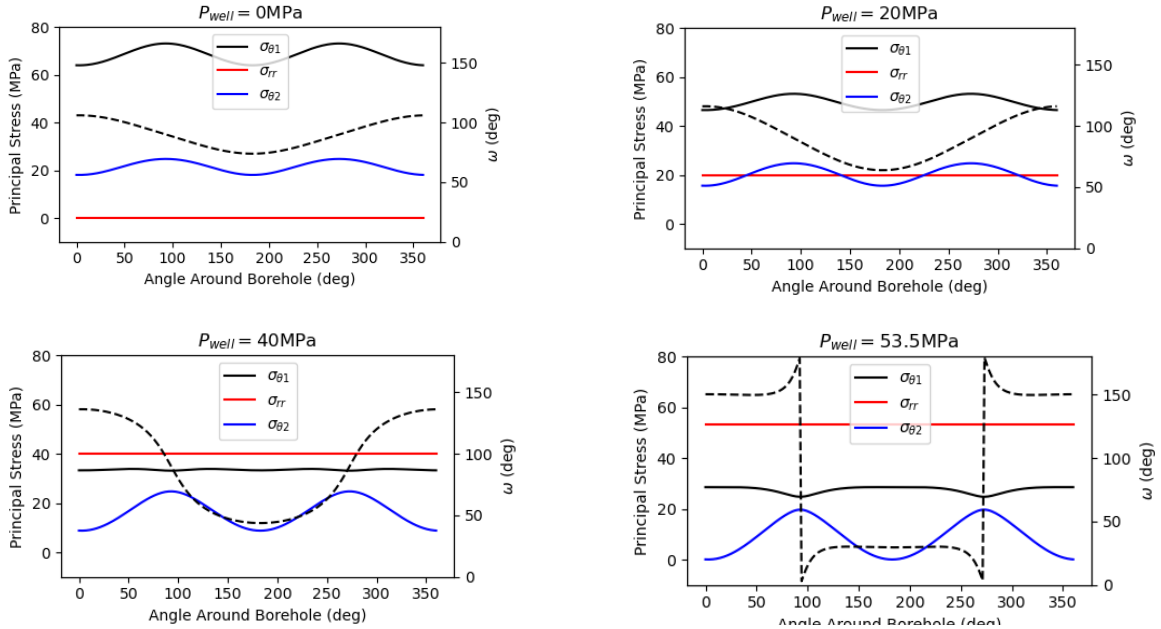

Figure 8.Plot of the principal stresses around the circumference of the borehole for the most likely stress conditions under the assumption that fractures are induced in TV4100 at the orientation where the stress is most tensile; σ_{rr} is the radial principal stress and is equal to the fluid pressure in the well; $\sigma_{\theta 1}$ is the most compressive of the tangential stresses while $\sigma_{\theta 2}$ is the least compressive; ω is the angle formed between the direction of $\sigma_{\theta 2}$ and a plane perpendicular to the well and is plotted with the dashed black line; the fluid pressure inside of the well for each plot is indicated above the plot

that if the rock strength were very low a fracture would be expected to form at the top and bottom of the well that is approximately 60° misaligned with the axis of the borehole (since 150°-90°=60°, and 90° represents a longitudinal fracture).

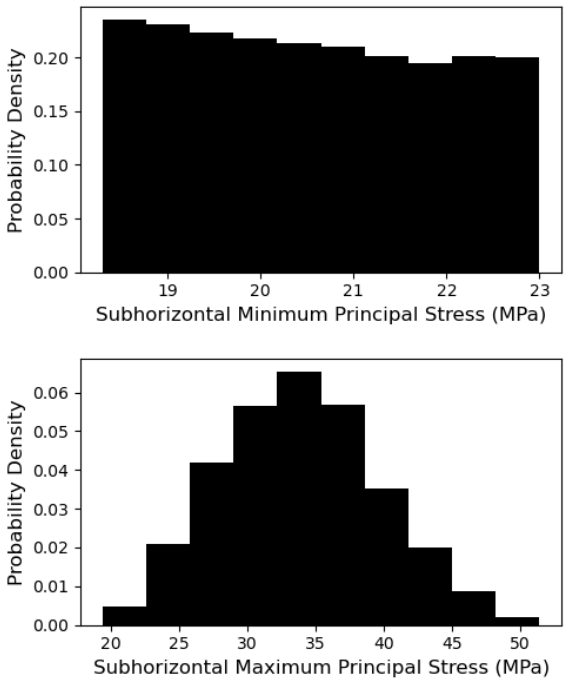

Figure 9. Posterior distribution for the magnitude of the minimum and maximum subhorizontal stresses under the assumption that fractures are induced at the orientation where the stress is most tensile

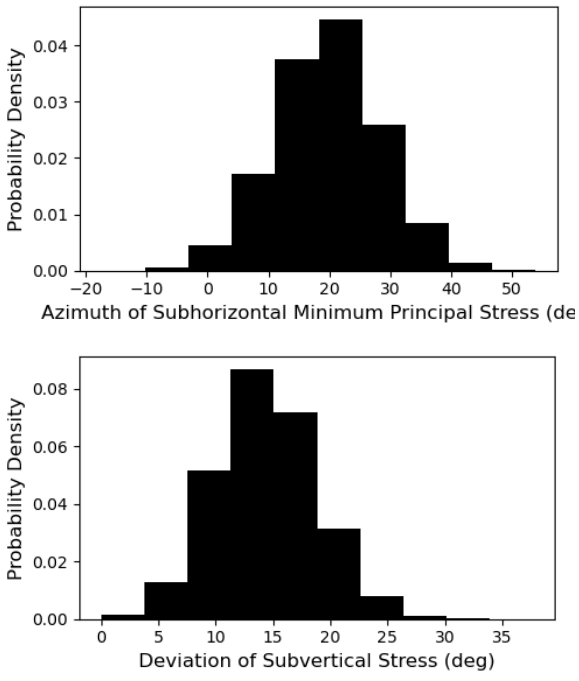

Figure 10. Posterior probability distribution for the azimuth of the minimum subhorizontal stress and the deviation of the lithostatic stress from vertical under the assumption that fractures are induced at the orientation where the stress is most tensile

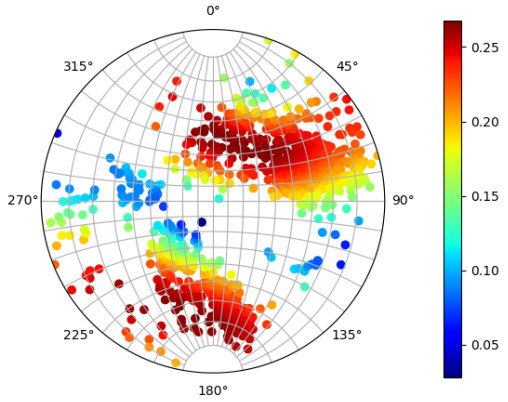

Figure 11. Equal angle lower hemisphere projection of poles of identified fractures in E2-TC, colored according to the mean shear-to-normal stress ratio under the assumption that fractures are induced in TV4100 at the orientation where the stress is most tensile

Figure 11 shows a stereonet plot of the lower hemisphere projection of the poles of fractures identified from E2-TC logs. The glyph associated with each fracture is colored according to the mean shear-to-normal stress ratio on the fracture plane. The shear to normal stress was computed by projecting each MCMC stress realization to each fracture plane, and then computing the average value. Figure 12 contains plots describing uncertainty in the shear and normal stresses for the fracture that is most favorably oriented for shear slip in this stress hypothesis and within the geophysical monitoring zone. The geophysical monitoring zone is the zone of the well that has good coverage for the geophysical instruments installed in adjacent boreholes and is therefore the region of the test bed desired for stimulation.

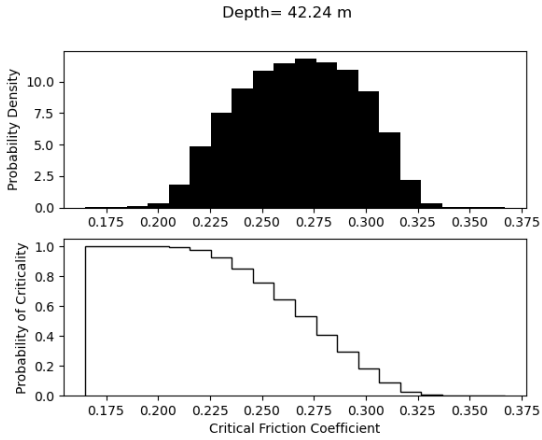

Figure 12. Plot of shear-to-normal stress ratio for the fracture at a depth of 42.24 m in well E2-TC, which has the most favorable stress state for shear failure; the upper plot is the probability density for the shear to normal stress ratio; the bottom plot is the survival function (1-cumulative distribution function), which indicates the probability, for each value of the friction coefficient, of the fracture sliding in shear if it had that value of friction coefficient and no cohesion; order of favorability is left to right, top to bottom

3.2. *Rock fabric-driven fracture orientation hypothesis*

To reflect this hypothesis, the sleeve fracture reopening pressure expected for each MCMC stress realization was computed by finding the packer pressure that would produce zero normal stress on the realization of the induced fracture orientation (consistent with the uncertain in observed fracture orientations). Figure 14 and Figure 15 show histograms of the MCMC realizations for the principal stress magnitudes and directions for this hypothesis. Note that the stress directions were not fixed as part of this assumption, but by fixing the orientation of the induced fractures and with the prior probability that prefers a vertically oriented lithostatic stress, the stress orientations produced by this hypothesis are closer to vertical/horizontal than with the stress-driven hypothesis.

This assumption changes not just the stress orientations, but also the stress magnitudes. This hypothesis results in a larger expected value for the maximum subhorizontal stress because a larger stress contrast is needed to result in an opening pressure on a fracture that is mis-oriented from the principal stress directions. Notably, using the most likely value of the stresses under this assumption, with the packer pressure at 20.1 MPa, when the fracture reopens, there is a tensile of 12.5 MPa stress in the direction that would produce a vertical fracture. Since no fracture of this orientation was observed in the stress measurement tests, this means that this stress hypothesis is only plausible if the rock tensile strength exceeded 12.5 MPa at every zone tested in TV4100.

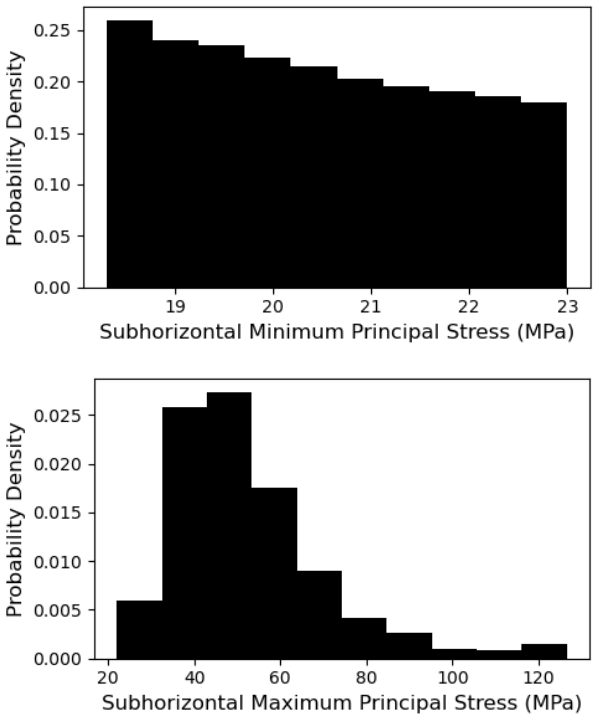

Figure 14. Posterior distribution for the magnitude of the minimum and maximum subhorizontal stresses under the assumption that fractures are induced at an orientation fixed by a plane of weakness in the rock fabric, not by the orientation where the stress is most tensile

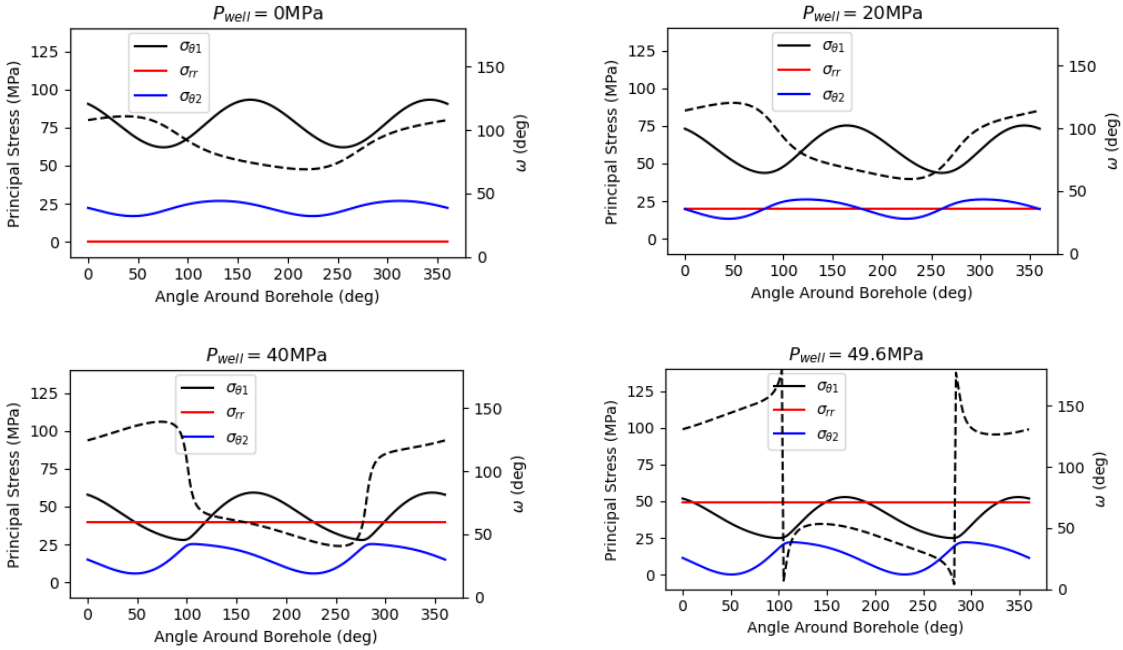

Figure 13. Plot of the principal stresses around the circumference of the borehole for the most likely stress conditions under the assumption that fractures are induced at an orientation fixed by a plane of weakness in the rock fabric, not by the orientation where the stress is most tensile; σ_{rr} is the radial principal stress and is equal to the fluid pressure in the well; $\sigma_{\theta 1}$ is the most compressive of the tangential stresses while $\sigma_{\theta 2}$ is the least compressive; ω is the angle formed between the direction of $\sigma_{\theta 2}$ and a plane perpendicular to the well and is plotted with the dashed black line; the fluid pressure inside of the well for each plot is indicated above the plot

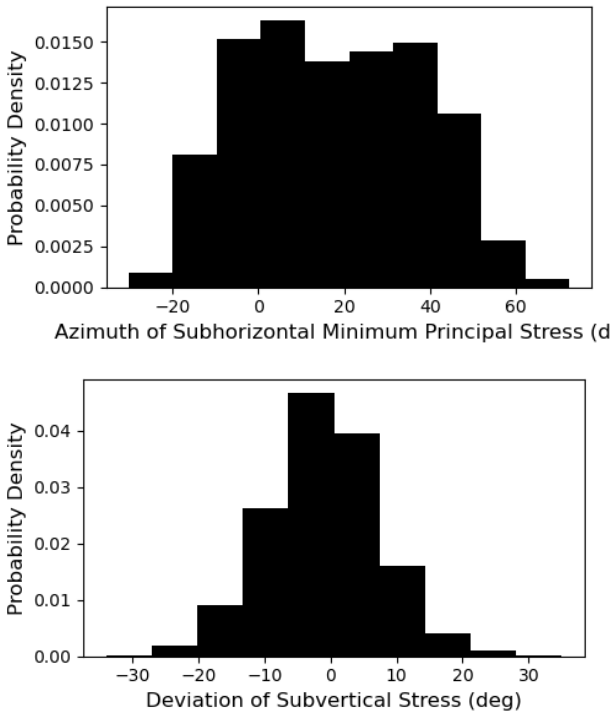

Figure 15. Posterior probability distribution for the azimuth of the minimum subhorizontal stress and the deviation of the lithostatic stress from vertical under the assumption that fractures are induced at an orientation fixed by a plane of weakness in the rock fabric, not by the orientation where the stress is most tensile

Figure 13 shows a plot of the stresses surrounding well E2-TC for the most likely stress state under this hypothesis as a range of well pressures. The plots in this figure indicate that a fluid pressure of 49.6 MPa (7194 psi) would be required to begin producing tensile tangential stresses on the surface of the borehole. Additional pressure above this value would be required to overcome the tensile strength of the rock and produce a fracture. With a fluid pressure of 49.6 MPa (7194 psi), where the tangential stress begins to become tensile, the location of the tensile component of stress rotated approximately 51° from the top and bottom of the well, measured as a positive rotation with respect to the down going axis of the well using a right-hand rule. The orientation of the tensile component of stress is 145° with respect to a plane perpendicular to the well. This means that if the rock strength were very low a fracture would be expected to form 50° from the top and bottom of the well that is approximately 55° misaligned with the axis of the borehole.

Like the stress-driven stress hypothesis, all stress realizations from the MCMC run were mapped to the fractures observed in E2-TC. Figure 16 shows a stereonet plot of these fractures with each fracture colored according to the mean shear-to-normal stress ratio. Figure 17 shows the histogram of the shear-to-normal stress ratio for the fracture with the highest expected shear/normal stress ratio to illustrate the uncertainty about this mean value.

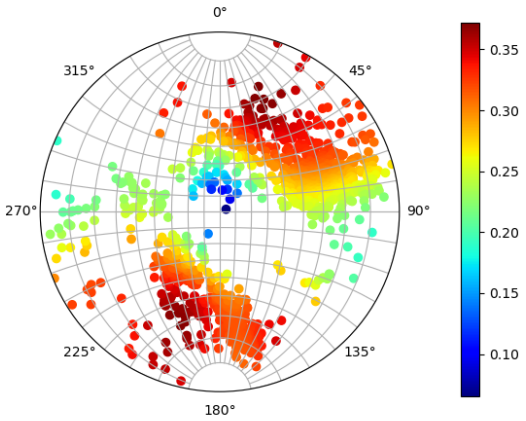

Figure 16. Equal angle lower hemisphere projection of poles of identified fractures in E2-TC, colored according to the mean shear-to-normal stress ratio under the assumption that fractures are induced at an orientation fixed by a plane of weakness in the rock fabric, not by the orientation where the stress is most tensile

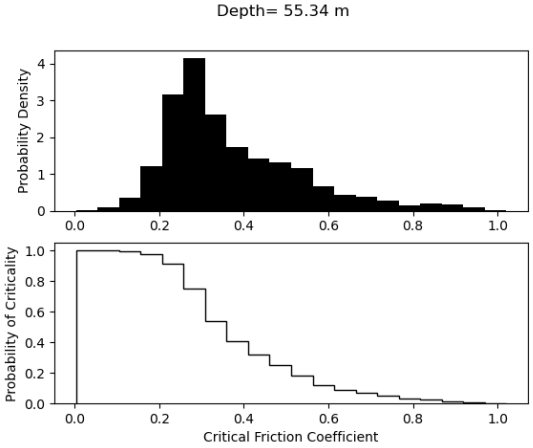

Figure 17. Plot of shear-to-normal stress ratio for the fracture with the most favorable stress state; the upper plot is the probability density for the shear to normal stress ratio; the bottom plot for each fracture is the survival function (1-cumulative distribution function), which indicates the probability, for each value of the friction coefficient, of the fracture sliding in shear if it had that value of friction coefficient and no cohesion; order of favorability is left to right, top to bottom

4. CONCLUSIONS

A stochastic Markov Chain Monte Carlo (MCMC) method was used to integrate all of the stress indicators identified in the EGS Collab Experiment 2 test bed and produce an estimate for the joint probability distribution of the principal stress magnitudes and directions. Two different hypotheses have been put forth to explain the significant and consistent deviation from vertical of the fractures induced in the stress measurement campaign. The first is that the fractures deviate from vertical because the principal stresses deviate from vertical/horizontal. The second is that the fractures are inclined because of a persistent plane of weakness at the observed orientation of induced fractures.

These two hypotheses were expressed as assumptions in two different runs of the MCMC algorithm, resulting in a probability distribution for the stress state reflecting each hypothesis. For each hypothesis, the stress realizations were used to compute the stress state around the planned stimulation well, E2-TC, as well as the expected tensile fracturing pressure and expected resulting fracture orientation. The stress realizations were also mapped to the fractures identified in image logs in this well and the probability distribution for the shear-to-normal stress ratio was computed for each fracture.

In general, the largest shear-to-normal stress ratios are relatively low, reflecting that even the most favorable fractures are far from failure. This is expected to make shear stimulation difficult in this test bed because it will require a substantial increase in fluid pressure within the fractures. Because the fractures also appear to have quite low hydraulic conductivity, it may not be possible to achieve such large pressure increases inside the fractures while avoiding the formation of tensile fractures.

Nonetheless, the fractures with the highest expected value of the shear-to-normal stress ratio are being targeted for the Experiment 2 shear stimulation test. The current plan is to hold several of these most-favorable fractures under a pressure below the minimum principal stress for days or weeks to give fluid pressure time to diffuse into the fracture. The fluid pressure for these long pressure holds has been chosen to be 15.2 MPa, which is approximately 83% of the lowest expected value for the minimum principal stress.

Because the fractures that are most favorable for shear are different for the two stress hypotheses, the results of the shear stimulation test may help to discriminate which of the hypotheses is correct. Furthermore, at least one tensile fracturing test is planned. Since the expected induced tensile fracture orientation is also different for the two stress hypotheses, this will also likely provide evidence that can test each hypothesis. The results of this test will also provide some test of the validity of the stress characterization and uncertainty quantification method used here, which will help to understand how it could best be applied to stimulation of deep/hot EGS reservoirs. Finally, the rigorous uncertainty quantification performed here will allow for a more robust and objective interpretation of the results of the shear stimulation experiment by reflecting the true uncertainty of the state of stress.

ACKNOWLEDGMENTS

This material was based upon work supported by the U.S. Department of Energy, Office of Energy Efficiency and Renewable Energy (EERE), Office of Technology Development, Geothermal Technologies Office, under Award Number DE-AC05-76RL01830 with PNNL and other awards to other national laboratories. Sandia National Laboratories is a multimission laboratory managed and operated by National Technology & Engineering Solutions of Sandia, LLC, a wholly owned subsidiary of Honeywell International Inc., for the U.S. Department of Energy's National Nuclear Security Administration under contract DE-NA0003525. This paper describes objective technical results and analysis. Any subjective views or opinions that might be expressed in the paper do not necessarily represent the views of the U.S. Department of Energy or the United States Government. The United States Government retains, and the publisher, by accepting the article for publication, acknowledges that the United States Government retains a non-exclusive, paid-up, irrevocable, world-wide license to publish or reproduce the published form of this manuscript, or allow others to do so, for United States Government purposes. The research supporting this work took place in whole or in part at the Sanford Underground Research Facility in Lead, South Dakota. The assistance of the Sanford Underground Research Facility and its personnel in providing physical access and general logistical and technical support is gratefully acknowledged. We also thank the crew from RESPEC, who directly supported both the core and wireline logging operations needed for this study.

REFERENCES

1. Bažant, Z.P., & Planas, J. (1998). Fracture and Size Effect in Concrete and Other Quasibrittle Materials (1st ed.). Routledge.
2. Burghardt, J., T. Doe, M. Ingraham, P. Schwering, C. Ulrich, W. M. Roggenthen, C. Reimers and EGS Collab Team (2020). "Integration of Shut-In Pressure Decline, Flow back, Hydraulic and Sleeve Re-Opening Tests to Infer In-Situ Stress." 54th U.S. Rock Mechanics/Geomechanics Symposium.
3. Chiaramonte, L., J. A. White and W. Trainor-Guitton (2015). "Probabilistic geomechanical analysis of compartmentalization at the Snøhvit CO2 sequestration project." Journal of Geophysical Research: Solid Earth **120**(2): 1195-1209.
4. Gelman, A., J. Carlin, H. Stern, D. Dunson, A. Vehtari and D. Rubin (2004). Bayesian Data Analysis, Chapman and Hall/CRC.
5. Kneafsey, T., Dobson, P. Ulrich, C., Hopp, C., Rodriguez-Tribaldos, V., Guglielmi, Y., Blankenship, D., Schwering, P., Ingraham, M., Burghardt, J., White, M., Johnson, T., Strickland, C., Vermeul, V., Knox, H., Morris, J., Fu, P., Smith, M., Wu, H., Ajo-Franklin, J., Huang, L., Neupane, G., Horne, R., Roggenthen, W., Weers, J., Doe, T., Pyatina, T. (2022). The EGS Collab Project - Stimulations at Two Depths. In *Proc. 56th US Rock Mechanics/Geomechanics Symposium*, Santa Fe, NM. American Rock Mechanics Symposium
6. Masoumi, H. (2020). Size effect of rock samples. In: Scale-Size and Structural Effects of Rock Materials, edited by S. Wang, H. Masoumi, J. Oh and S. Zhang. Woodhead Publishing 2020

7. Norbeck, J. H., M. W. McClure, and R. N. Horne (2018). "Field observations at the Fenton Hill enhanced geothermal system test site support mixed-mechanism stimulation." Geothermics **74**: 135-149.
8. Peška, P. and M. D. Zoback (1995). "Compressive and tensile failure of inclined well bores and determination of in situ stress and rock strength." Journal of Geophysical Research: Solid Earth **100**(B7): 12791-12811.
9. Stetler, L. D. (2015). "Water geochemistry and pressure buildup in drill holes on the 4850-ft level at the Sanford Underground Research Facility." Proceedings of the South Dakota Academy of Science **94**: 317-327.
10. Ulrich, C., Dobson, P., Kneafsey, K., Roggenthen, W., Uzunlar, N., Doe, T., Neupane, G., Artz, T., Dobler, K., Schwering, P., Smith, M., Burghardt, J., (2022). Characterizing rock fractures and physical properties for Experiment 2 of the EGS Collab Project, Sanford Underground Research Facility. In *Proc. 56th US Rock Mechanics/Geomechanics Symposium*, Santa Fe, NM. American Rock Mechanics Symposium
11. Zoback, M. D., C. A. Barton, M. Brudy, D. A. Castillo, T. Finkbeiner, B. R. Grollimund, D. B. Moos, P. Peska, C. D. Ward and D. J. Wiprut (2003). "Determination of stress orientation and magnitude in deep wells." International Journal of Rock Mechanics and Mining Sciences **40**(7-8).